HHS Public Access

Author manuscript

Ann Biomed Eng. Author manuscript; available in PMC 2020 February 21.

Published in final edited form as:

Ann Biomed Eng. 2017 November ; 45(11): 2592–2604. doi:10.1007/s10439-017-1896-3.

A wireless pressure sensor for continuous monitoring of intraocular pressure in conscious animals

Simon A. Bello[1], **Christopher L. Passaglia**[2,3]

[1]Department of Electrical Engineering, University of South Florida, Tampa, FL, 33620

[2]Department of Chemical & Biomedical Engineering, University of South Florida, Tampa, FL 33620

[3]Department of Ophthalmology, University of South Florida, Tampa, FL 33620

Abstract

An important aspect of eye health in humans and animal models of human diseases is intraocular pressure (IOP). IOP is typically measured by hand with a tonometer, so data are sparse and sporadic and round-the-clock variations are not well characterized. Here we present a novel system for continuous wireless IOP and temperature measurement in small animals. The system consists of a cannula implanted in the anterior chamber of the eye connected to pressure sensing electronics that can be worn by rats or implanted in larger mammals. The system can record IOP with 0.3 mmHg accuracy and negligible drift at a rate of 0.25 Hz for 1–2 months on a regulated battery or indefinitely at rates up to 250 Hz via RF energy harvesting. Chronic recordings from conscious rats showed that IOP follows a diurnal rhythm, averaging 16.5 mmHg during the day and 21.7 mmHg at night, and that the IOP rhythm lags a diurnal rhythm in body temperature by 2.1 hours. IOP and body temperature fluctuations were positively correlated from moment-to-moment as well. This technology allows researchers to monitor for the first time the precise IOP history of rat eyes, a popular model for glaucoma studies.

Keywords

glaucoma; rat; eye; telemetry; wireless; energy harvesting

INTRODUCTION

Intraocular pressure (IOP) measurement is important for diagnosing and monitoring glaucoma[13], the second leading cause of blindness in the world. IOP that is too high or too low for a sustained period can permanently damage the optic nerve or detach the retina, so maintaining IOP in a clinically normal range is the focus of most treatments of the disease[10]. The gold standard of IOP measurement is applanation tonometry, which estimates pressure from the amount of force needed for a probe to flatten a prescribed area of the cornea. The method is noninvasive and accurate, but it requires time and training since readings are made

Corresponding author: Dr. Christopher L. Passaglia, Department of Chemical and Biomedical Engineering, University of South Florida, 4202 E Fowler Ave, Tampa, FL 33620. Phone: 813-974-7140, passaglia@usf.edu.

by hand. The sparse and sporadic yield of data limits the usefulness of tonometry for tracking IOP dynamics, which can fluctuate at multiple time scales in normal and glaucomatous eyes due to posture changes, blood pulsations, and biological rhythmns[1,2,4,8,15–18,29]. Much research effort has therefore been directed at developing technologies for round-the-clock IOP measurement.

A variety of custom-made and commercial pressure sensors have been designed or adapted for use in animals. Among the first were contact lenses embedded with strain gauges to detect pressure-induced changes in scleral or corneal curvature[6,9], and one is now approved for clinical use (Sensimed Triggerfish®)[17,18]. At present the technology is only suitable for humans or animals with similar size eyes, and it can only report relative changes with arbitrary units since IOP is not sensed directly. Two invasive approaches have been taken for absolute IOP measurement. One is to implant a pressure-sensitive electromechanical circuit inside the eye[5,25,26], and the other is to cannulate the eye with a tube connected to an external pressure transducer[3,7,14,19]. Intraocular IOP sensors have progressed to point of human clinical trials (Implandata EyeMate®)[20], but they too are constrained by size to large eyes. The technology also relies on a handheld unit for power transmission that hinders its usefulness for round-the-clock data collection. Eye cannulation has met with greatest success. Since pioneering work in rabbits over 20 years ago[19], IOP has been recorded continuously for weeks from animals as small as mice[14]. Nearly all studies to date used commercial telemetry systems built to measure standard physiological signals like temperature, bioelectrical potentials, and blood pressure. The systems are convenient and robust, but they were not designed for long-term IOP recordings. They generally provide moderate accuracy at physiological IOP levels, require frequent recalibration due to battery-related drifts in output, operate intermittently in order to conserve power and maximize recording duration, and employ cannulas that are too large for the eyes of small animals commonly used for glaucoma research.

Here we present a novel wireless telemetry system for continuous monitoring of IOP and body temperature in rats and potentially larger animals. Two methods of system powering are described: active battery regulation and radio-frequency (RF) energy harvesting. The two methods offer accurate round-the-clock measurement for months to animal lifetime without drift in performance. We evaluate and quantitatively characterize the properties of the technology in conscious rats.

MATERIALS AND METHODS

Animal preparation

Experiments were performed on adult Brown-Norway rats (300–400 g) housed in a temperature-controlled room (21°C) under a 6:00am-6:00pm light-dark cycle and fed a standard daily diet. All procedures were approved by the Institutional Animal Care and Use Committee of the University of South Florida in accordance with NIH guidelines.

System design

The IOP telemetry system (figure 1A) consists of a fine polyimide cannula (100 μm ID, 140 μm OD), a custom-made plastic coupler, connection tubing, and a sealed plastic box (23 × 23 × 12 mm) that houses a piezoresistive pressure transducer with a silicone-gel coated membrane (TBP Series, Honeywell, Morristown, NJ), temperature sensor, amplifiers, microcontroller, wireless transmitter, and power circuitry (figure 1B). The cannula is filled with artificial aqueous humor or physiological saline and surgically implanted in the anterior chamber of the eye[3]. It is fed subdermally to the input port of the coupler, which is affixed to the skull with bone screws (figure 1C). The coupler (Delrin®, Interstate Plastics, Sacramento, CA) was designed for head mounting on rats using CAD software (SolidWorks, Waltham, MA) and machined in house. The output port of the coupler is connected to a clear 16G PTFE tube surrounded by a metal spring that prevents tube kinking. The tube conducts IOP to the pressure transducer inside the box (figure 1D), and the box attaches to a custom-fit vest that the animal wears (figure 1E). A soft undergarment may be worn under the vest to prevent skin irritation.

System powering

Two versions of the IOP telemetry system were developed that use different power circuitry. We shall refer to them as the battery regulated system (BRS) and wirelessly powered system (WPS). The BRS (13 g) runs on a coin-cell battery (Duracell CR2032), and embedded circuitry regulates battery output over time so as to maintain a constant supply voltage of 3.3 V. The microcontroller is programmed to take 20 pressure readings at 50 Hz every 20 seconds and transmit the average IOP and temperature data to a PC laptop equipped with a low-energy Bluetooth (BLE 4.0) receiver, which can synchronize with up to 8 telemetry systems simultaneously in a ~2 m radius. A custom LabVIEW (National Instruments, Austin, TX) program stores and displays transmitted IOP and temperature data for each implanted animal. Data transmission rate and distance can both be increased to suit experiment needs at the expense of battery life.

The WPS (11 g) draws power wirelessly from an energy harvesting circuit comprised of a custom-designed RF power antenna, RF harvester, and energy storage unit (figure 1F). The custom antenna collects 915 MHz energy generated by two 1 W orthogonally-oriented RF emitters (TX91501, Powercast, Pittsburg, PA) located atop the rat's cage (35 × 25 × 20 cm). The cage, feeding rack, and water bottle (RS1-H, Innovive, San Diego, CA) are all made of plastic to reduce RF signal scatter and reflection that would attenuate power reception. The combination of cage design, unique antenna shape, and transmitter placement allows the system to always harvest energy irrespective of animal location or orientation in space. The RF harvester then converts collected energy to a DC voltage that charges the storage unit while special circuitry feeds stored energy to the rest of the system at a constant supply voltage of 3.3 V. Since power reception will vary as animals move, the storage unit is charged and drained during experiments in a regulated manner. If the stored level is between 3.2 and 4.5 V, the WPS is programmed to acquire 20 pressure readings at 50 Hz every 4 seconds and transmit the mean IOP, sensor temperature, and stored voltage wirelessly to the Bluetooth-enabled computer. If the level exceeds 4.5 V, the WPS instead streams pressure data to the laptop at 250 Hz until stored voltage is drained below this level. A 10-sec epoch

consumes approximately 0.1 V so the data burst prevents overcharging the storage unit beyond its maximum energy rating in addition to providing a short high-resolution IOP record. If the level dips below 3.2 V, the WPS just harvests energy. No data is acquired until stored voltage is replenished.

Bench testing

The long-term stability of the IOP telemetry system was determined by exposing the BRS and WPS to constant hydrostatic pressure for 90 days. The pressure was supplied by a reservoir of saline reservoir connected via a three-way stopcock to the system and to a mercury manometer. The reservoir was sealed to prevent evaporation, and fluid levels were periodically checked to ensure applied pressure did not change. Since the WPS is fixed in position, a single RF emitter at a distance of 20 cm was used for power. For comparison, data were also collected from a system that did not have circuity for battery power regulation. The battery unregulated sensor (BUS) was otherwise identical to the BRS. Pressure records were analyzed by linear regression to quantify any drift in system output. System power consumption (P) was calculated via the formula: $P = V \cdot I$, where V is supply voltage and I is current drained during operation. Current drainage for data collection and wireless transmission was measured with the system connected to a DC power supply and data acquisition board (USB-6008, National Instruments, Austin, TX).

WPS power transfer was quantified by mapping the radiation pattern of the two RF emitters with the system mounted on a cadaver rat. The rat was moved along a 60 × 60 cm grid divided into 36 squares. At each square the animal was turned a full revolution, and the power absorbed by the RF antenna was measured with a spectrum analyzer (N9915A, Agilent Technologies, Santa Clara, CA). Maximum and minimum power levels were recorded at each grid location with the RF emitters placed first at a height of 20 cm and then 60 cm.

IOP measurement and analysis

System performance in conscious rats was evaluated in 10 experiments. Details of the cannula implantation procedure were described previously[3]. In short, animals were anesthetized with ketamine (50 mg/kg IP) and xylazine (7 mg/kg IP), with supplemental injections given as needed. The head was secured in a stereotaxic apparatus, and the pupils were dilated with 1% cyclopentolate. An incision was made in the conjunctiva of one eye and the head. Tissue overlying the skull was retracted, bone was cleaned with 3% hydrogen peroxide, and the coupler was affixed with a stainless steel screw (#303, J.I. Morris, Southbridge, MA) in each bone plate. The cannula was fed into the coupler, sealed in place with cyanoacrylate, and tunneled subdermally to the eye. A translimbal hole was made with a 33G needle, and 1 μL triamcinolone acetonide (Triesence, Alcon, Fort Worth, TX) was injected into the anterior chamber to counteract inflammation. The cannula tip was passed through the hole and sutured to the sclera. The spring-enclosed tubing was then connected to the coupler and wireless pressure sensor. The coupler was covered in bone cement, and incisions were closed with sutures. Every 12 hrs for 3 days after surgery, animals were given carprofen (5 mg/kg, IM) for pain mitigation. Once daily for the first 4 days and sporadically thereafter, the system was disconnected and the cannula tip was flushed with 25%

moxifloxacin ophthalmic solution (Vigamox, Alcon, Fort Worth, TX) to maintain lumen patency during wound healing. Data were discarded after tip flushing until readings stabilized at prior levels (<1 hr). IOP readings were validated in 3 experiments by temporarily anesthetizing the animal and cannulating the implanted eye with a 33G needle connected via a three-way stopcock to a reservoir of physiological saline and an inline pressure transducer (5110, Stoelting, Wood Dale, IL). System and transducer outputs were compared as reservoir height was varied from 5 to 45 mmHg. IOP readings were evaluated in other experiments against tonometry (Tono-Pen XL, Medtronic, Sarasota, FL). A total of 6 tonometer measurements were made from each eye 2–3 times per week with the rat under isoflurane anesthesia.

Signals recorded by the IOP telemetry system could contain large blips from animal feeding or grooming movements. Records were cleaned of blips by flagging pressure data that deviated more than 20 mmHg from adjacent points and removing the outliers along with the preceding and succeeding points. Only records with >99.9% raw data are reported here. The presence of a diurnal rhythm was examined by calculating the mean IOP in 1-hr bins over a 24-hr period and in 12-hr blocks averaged over the entire record. The blocks corresponded to day and night phases of the light-dark cycle. Statistical significance was assessed by a two-sample t-test with an alpha level of 0.05 using SigmaPlot software (San Jose, CA). Results are expressed in terms of mean ± standard deviation (SD).

Temperature measurements

The telemetry system is equipped with a temperature sensor for body temperature measurement. At present, the system is too large for subdermal implantation in rats but it might give an indirect measure of body temperature from atop the back. To evaluate this, 3 animals were anesthetized with isoflurane and placed belly-down on a heating pad in a temperature-controlled room. Core body temperature was recorded by a rectal thermometer and varied between 35 to 39 °C by the heating pad. Temperature sensor readings were linearly regressed to the thermometer data, and the regression slope and offset were used to calibrate system output for a given rat. IOP and temperature records from conscious animals were correlated using a custom MATLAB program. Observed periodicities in correlation data were fit by a sinusoid function: $f(x) = a \cdot sin\left(\frac{2\pi \cdot x}{b} + c\right)$. Statistical significance was assessed via a bootstrap approach; in which, the probability distribution of chance correlation was estimated by correlating temperature and IOP data with 1000 randomly shuffled versions of the data.

RESULTS

System properties

The functional properties of the battery-operated and batteryless versions of the IOP telemetry system were characterized by applying constant hydrostatic pressure to the sensor for several weeks. Figure 2A (top) shows the stored voltage when the system was powered by an unregulated 3 V lithium-ion battery. The voltage record exhibits a triphasic behavior typical of this battery (n = 6), falling rapidly in the first days from 3.3 V to an operating level of ~3 V which drains gradually and then more quickly over following weeks to ~2.8 V at

which point the battery runs out and the system shuts down. Figure 2A (bottom) shows that the unsteady voltage supply caused sensor output to drift with time, wandering slowly downward and then upward over the first three weeks before settling at a roughly stable value until shutdown. Pressure readings also became more variable toward the end of battery life, increasing from 0.23 to 0.33 mmHg in SD. Figure 2B shows that drift in sensor output was eliminated by battery-regulating circuitry that holds the supply level steady at 3.3 V. Pressure records for the BRS exhibited negligible drift and less noise (slope = 0.01 ± 0.02 mmHg/week, SD = 0.18 mmHg, n = 3). The stability came with the cost of power consumption as regulating circuits reduced battery life (BUS: 38 ± 1 days, BRS: 28 ± 3 days, sample rate: 0.25 Hz). Figure 2C shows that the system can output stable pressure readings for months, and presumably for the life of the animal, when powered by energy harvesting circuitry. Pressure records for the WPS also showed negligible drift and low noise (slope = 0.002 ± 0.001 mmHg/week, SD = 0.15 mmHg, n = 3) due to regulating circuitry that held constant the supply voltage to the pressure sensor. Stored voltage actually increased from a pre-charge of 3.4 V to a sustained level around 4.1 V. Such behavior is quite unlike battery-powered devices. The properties of the BRS and WPS are summarized in Table 1.

The near-monotonic rise in stored voltage indicates that the WPS harvested more energy than it consumed. This will not always happen when the system is placed on animals that move. Figures 3A and 3B show power consumption profiles during one cycle of IOP and temperature data collection and data transmission, respectively. The system was configured to take 20 readings per cycle. It draws 12.5 mW for 1 ms for initialization and each reading and 1.3 mW between readings. It then draws 12.5 mW for 60 ms to compute and transmit the average. Power consumption is insignificant (12 μW) at other times, so the integral gives a total energy expenditure of 1.7 mJ per cycle. This is the minimum amount of energy the WPS must harvest every 20-s cycle period to maintain operation. How much it actually harvests will depend on the RF emission field and time-varying location and orientation of the RF antenna within that field. Power transfer levels were spatially mapped by translating and rotating a cadaver rat wearing the WPS. Figures 3C and 3D respectively plot the minimum and maximum power received over 360° of antenna rotation in and around the animal's cage with RF emitters at a height of 20 cm. Power reception was strong throughout the cage, with peak levels of 12.6 mW. It weakened toward cage corners but still exceeded 1 mW for suboptimal antenna orientations. This amounts to >20 mJ per cycle, which is more than ample for the system to record IOP indefinitely at stated rates. The cycle could even be shortened to seconds with little risk of system shut down. The RF emitters were further elevated to determine the height at which the WPS ceased operating. Minimum power transfer levels within the cage fell to 0.15 mW (or <3 mJ per cycle) at 60 cm (not shown), so the batteryless design is limited in application to rodents at present, and perhaps rabbits if the cycle period is lengthened to reduce power transfer demands.

Figure 3E shows the energy harvested over two weeks by the WPS on a conscious rat with RF emitters positioned atop the cage. Stored voltage fluctuated as the animal roamed around (inset) but never dipped below the 3 V operating minimum. It hovered mainly around 4.5 V since the system was programmed to use excess power above this level to stream data at high rate so that fast IOP fluctuations could be monitored. Table 2 summarizes WPS performance in this and two other animals. Data collection was interrupted only twice across

all experiments by low power level. The longest interruption lasted 33 mins due to the rat resting in posture and location within a dead zone for energy harvesting. Storage levels were otherwise sufficient to trigger data bursts every 2–10 minutes.

IOP recordings in awake behaving rats

Once the IOP telemetry system was optimized for mounting on awake behaving rats, data were collected round-the-clock from 10 animals. Experiments lasted until fibrotic buildup eventually clogged the cannula tip. The fibrosis caused readings to decrease and go negative, indicating the sensor became sealed off from atmospheric pressure. Most experiments (n = 8) yielded data for at least two weeks and some (n = 4) for about a month. In no experiment did the system itself fail. Sensor accuracy was assessed in a subset of experiments by temporarily anesthetizing the rat, cannulating the implanted eye with a needle connected to a manometer and pressure sensor, and stepping IOP manometrically to normal and glaucomatous levels (figure 4A). The system tracked the applied pressure at all levels tested (R = 0.99, measurement SD = 0.27 mmHg, n = 3).

Figure 4B plots the IOP recorded over two days in a conscious rat. It can be seen that readings fluctuated on multiple time scales, ranging from minutes to days. Pulsatile fluctuations due to heart beats or eye movements, if present, were not detected by the system (supplemental figure S1). IOP varied in this animal from 7 to 26 mmHg about a mean of 15.4 ± 4.1 mmHg. Not all the variability can be attributed to the eye, however, as IOP is conducted to the system by a flexible fluid-filled tube. To estimate how much variability is spurious, the cannula tip was cut at the limbal insertion point. Figure 4C plots a two-day pressure record from the same animal after opening the cannula to air. The mean reading dropped instantly to 0 mmHg and the slow diurnal oscillation was eliminated, indicating that these components of the IOP record originated within the eye. The fast fluctuations remained but were reduced in amplitude (SD = 1.5 mmHg, n = 3). They are consistent with body posture changes, which would be expected to cause pressure variations up to 3 mmHg based on the distance of the system sensor from the eye (~45 mm). Raw IOP records were therefore smoothed to attenuate fluctuations due to head elevation and rotation. The temporal characteristics of the smoothing filter were defined by analyzing the statistical properties of the intraocular and extraocular pressure signals. Figure 4D plots the auto-correlation function of the two records, both of which have a sharp peak at 0 lag. The peak width indicates that the signals are correlated in time for ±30 min so IOP records were smoothed using a 1-hr lowpass filter.

Figure 5A shows a filtered IOP record from an awake behaving rat implanted for a month with the wireless system. The IOP of this animal fluctuated about a mean level of 17.6 ± 2.9 mmHg that was stable for the duration of the experiment. The fluctuations waxed between week-long intervals of irregularity and 24-hr periodicity for reasons that were not investigated. Figure 5B plots IOP data collected sporadically by hand with a TonoPen tonometer from this animal. Tonometer readings averaged 18.5 ± 4.2 mmHg for the implanted eye, which was not significantly different from the non-implanted eye (19.8 ± 2.4 mmHg, p = 0.07) nor the overall average IOP measured by the system (p = 0.26). The readings were positively correlated with system output recorded concurrently (figure 5C),

though consistently higher by 1.5 mmHg ($p = 0.007$) due to the tonometry procedure[19]. Figures 5D and 5E show filtered IOP data from two additional experiments that represent the extremes of IOP variation across implanted rats, which ranged from a weak and irregular fluctuation pattern to a pronounced and persistent diurnal rhythm.

The IOP rhythm was examined in further detail. Figures 6A and 6B show a 24-hr segment of the IOP record of an implanted rat and the hourly average over one week, respectively. IOP in this animal averaged 17.1 ± 1.6 mmHg during the day phase of the light-dark cycle and increased over the course of a few hours around lights off to 21.2 ± 2.0 mmHg during the night phase. Figure 6C summarizes the daytime and nighttime IOP levels for all implanted animals. Only one did not show a detectable rhythm. The mean day-night difference for rhythmic animals was 5.1 ± 1.4 mmHg.

Temperature recordings

The ability of the telemetry system to track rat body temperature from atop the back was examined in 3 experiments by resting anesthetized animals on a heating pad and varying pad settings. Figure 7A plots the temperature data collected concurrently by the system (T_{sensor}) and by a rectal thermometer (T_{body}). Linear regression of the datasets yielded an average slope of 1.39 ± 0.06. The small SD indicates the system can sense relative changes in body temperature. Regression intercepts, on the other hand, differed significantly due to assorted possible extraneous factors such as animal weight, vest fitting, and placement location. The system must therefore be calibrated to each rat and conditions must remain stable to correctly infer absolute body temperature.

Figure 7B shows two weeks of temperature data recorded by the BRS and WPS from an animal in temperature controlled housing. The data are expressed as *estimated body temperature* (T^*_{body}) based on system calibration curves. They are an estimate because sensor offset was not monitored and may have drifted over time. The offset appeared fairly stable though in most experiments (slope = 0.01 ± 0.03 °C/week, n = 5), with the illustrated WPS record being the lone exception. Mean temperature readings were not statistically different for the two systems (BRS: 37.8 ± 0.4 °C, WPS: 37.2 ± 0.4 °C, n = 6), even though the WPS is powered by a RF emitter that radiates near-field heat. Figure 7C shows a temperature record from another animal that was temporarily anesthetized without heat support on two occasions (bars). It can be seen that T^*_{body} dropped under anesthesia and returned afterwards to baseline, verifying that the system tracked real-time changes in rat body temperature. Auto-correlation analysis revealed a diurnal fluctuation in T^*_{body} (figure 7D). Sinewave fits of the correlation data yielded an average period of 24.5 ± 1.1 hrs across animals (n = 5). Cross-correlation analysis indicated that the temperature and IOP rhythms were nearly synchronous (figure 7E). Sinewave fits gave an average phase difference of 2.1 ± 0.4 hrs, with the temperature rhythm leading the IOP rhythm. The analysis also revealed a narrow peak in correlation that was offset slightly from zero (figure 7F). The mean time lag was 0.09 ± 0.04 hrs, meaning that temperature changes were often followed after a few minutes by IOP changes. The peak and periodic correlations were not artefactual because they were eliminated by randomly shuffling the temperature data.

DISCUSSION

In this study a new telemetry system is described for round-the-clock monitoring of IOP and body temperature in awake behaving rats and possibly larger animals. Battery-powered and batteryless versions of the system were developed, each of which offers certain advantages. The battery-powered system is simple to implement and low in cost because no external equipment is necessary besides a Bluetooth-enabled computer for data reception and storage. The system is implantable, though not in small animals like a rat. It is best suited for short-term IOP recordings since battery power lasts ~1 month. The exact lifespan depends on data collection rate, which is programmable by the user. Recording time can be extended indefinitely by battery replacement if the system is not implanted and worn like a backpack, as described here. The batteryless system is more complicated and costly to set up because special cages and equipment are required to provide steady wireless power to an object that can rotate and translate over a wide area. The advantage is the system can run indefinitely with ample power to perform additional functions besides IOP and temperature measurement.

Long-term recordings with the telemetry system revealed that rat IOP is not constant but rather varies dynamically by several mmHg. While some of the variation is a product of the backpack configuration, IOP was observed on many occasions to suddenly change even when the animal was stationary. These spontaneous fluctuations may play a role in glaucoma pathophysiology as well as mean IOP, and this technology provides a means of characterizing their statistical properties in small animals. Rat IOP records did not show heart-beat pulsations, unlike those of rabbits and monkeys[7,19]. We do not think they were mechanically filtered by sensor dynamics or system tubing since they also were not seen in calibration experiments that directly cannulated the eye with a needle (figure 4A). The pulsations were ~1 mmHg in monkey and 0.5 mmHg in rabbit so perhaps their amplitude scales with eye size and they are too small to detect in rat. Rat IOP was found to exhibit a diurnal rhythm, cycling between low daytime levels and high nighttime levels. A similar IOP rhythm has been observed in mice[14], rabbits[19], and humans[15–18] but not primates[7]. The day-night difference was 5mmHg in agreement with tonometry findings in rats[22]. The IOP rhythm was near synchronous with a diurnal rhythm in rat body temperature. The correlation was not a byproduct of pressure sensor electronics, which are thermally compensated (0.009 mmHg/°C from 10–50 °C). The temperature rhythm likely derived from the animal, although the system was outside the body, since room temperature was regulated and readings were highest at night when the room would otherwise be coldest. The nightly temperature increase is consistent with prior reports in rat[24].

Relation to existing technologies

Two commercial wireless systems have been used for continuous IOP measurement to date. The most common is the DSI system (C20 and C40), which has a battery life of 1–2 months and accuracy of ±3 mmHg according to the manufacturer. The other is the Konigsberg Instruments system (T30F-13B), which has an accuracy of 0.4 mmHg and can record IOP, ECG, and body temperature at 500 Hz for up to 9 months[7]. The Konigsberg system has significant performance advantages over the DSI system but is much too large and heavy for

small animals. The telemetry system introduced here is comparable to the Konigsberg system in accuracy and sample rate and comparable to the DSI system in size (1.4–5.9 cm^3) and weight (2.2–8 g). It cannot acquire multiple channels of physiological information but does offer three principle benefits. Firstly, the BRS and WPS provide constant power to the pressure sensor so readings are stable. Both commercial systems experience artificial drift in output of 6–17 mmHg/month due to unregulated battery drainage. To correct the drift they must be recalibrated every few weeks by inserting a needle into the eye, which puts ocular health at recurrent risk. Secondly, the cannula is small enough that it can be implanted for months in the narrow iridocorneal angle of rat eyes without significantly damaging intraocular tissues[3]. And thirdly, the WPS system can record IOP round-the-clock for weeks on end while data collection is intermittent with commercial systems due to recalibration, powering, and storage memory issues.

More generally, wireless powering solutions have been explored for various types of biological sensors. Most applications have sought to transfer energy via electromagnetic coupling between an implanted microcoil and an external source. The inductive coupling approach works well in near-field, where the source and power receiver are stationary and separated by a few cm[11,23,27]. However, it generally yields only a few hundred μW of power in the mid-field range of a small animal cage[11]. Higher transfer levels have been achieved in freely-moving rodents using specialized power-radiating enclosures[21,28], but not for sustained periods as the enclosures were not designed for animal housing or dissipating heat. In addition, power levels exceeded regulatory safety thresholds set by the IEEE[12]. The WPS can harvest up to 12 mW of power from RF emission fields that the Federal Communications Commission (FCC) deems safe for humans within a cage approved for rat housing.

Current limitations of system

A principal limitation of the IOP telemetry system is pressure sensor location. While the backpack design simplifies device troubleshooting and battery replacement, motion artifacts are introduced into pressure data. Horizontal head rotation can cause signal fluctuations due to tube kinking, the magnitude of which was greatly attenuated by encasing the tube in a stiff spring. Meanwhile, vertical head and posture movements cause signal fluctuations due to changes in fluid column height between the eye and sensor. This limitation is common to all catheter-based pressure sensors, as evidenced by the marked variability in some IOP studies[14]. It is least a problem for the Konigsberg system as the pressure sensor is separate from system electronics and mounted to supraorbital bone, which curtails tube kinking and minimizes fluid height differences. Also, back placement works for rats but probably not for large animals like monkeys that could damage or disconnect the system with their long reach. For the next iteration, the plan is to eliminate the coupler, shrink the footprint further, and mount the entire system to the skull to remove motion artifacts.

A secondary limitation is cannula tip patency, especially in small rodent eyes. While cannula implantation in the anterior chamber of the eye provides direct access to IOP and avoids inflammation and retinal damage often seen in intravitreal implants, the tip is subject to clogging from iris tendrils or fibrotic responses from healing tissues. Tendril formation can

be avoided with surgical practice and careful shaping of the cannula tip so it does not touch the iris[3]. Fibrotic responses, once initiated, are more challenging to resolve. It was found that the first days after implantation are especially important to the long-term success of an IOP recording, and it was often helpful to flush the cannula with a small volume of fluid as the wound healed to prevent tissue from growing along and into the tip. Once healing was complete, the system could be left to record IOP for weeks with minimal intervention.

Supplementary Material

Refer to Web version on PubMed Central for supplementary material.

ACKNOWLEDMENTS

The work was supported by NIH grant R21 EY023376 and a Thomas R. Lee Award from BrightFocus Foundation. The authors thank Mr. Dan Capecci for assistance with wireless communication programs. The following intellectual interests are declared: U.S. patents 9022968B2 and 9314375B1.

REFERENCES

1. Akaishi T, Ishida N, Shimazaki A, Hara H, Kuwayama Y. Continuous monitoring of circadian variations in intraocular pressure by telemetry system throughout a 12-week treatment with timolol maleate in rabbits. J. Ocul. Pharmacol. Therap 21 436–444. 2005. [PubMed: 16386085]
2. Asrani S, Zeimer R, Wilensky J, Gieser D, Vitale S, Lindenmuth K. Large diurnal fluctuations in intraocular pressure are an independent risk factor in patients with glaucoma. J. Glaucoma 9 134–142. 2000. [PubMed: 10782622]
3. Bello SA, Malavade S, Passaglia CL. Development of a smart pump for monitoring and controlling intraocular pressure. Ann. Biomed. Eng 1–13. 2016. [PubMed: 26620776]
4. Bengtsson B, Leske MC, Hyman L, Heijl A. Fluctuation of intraocular pressure and glaucoma progression in the early manifest glaucoma trial. Ophthalmol. 114 205–209. 2007.
5. Collins CC. Miniature passive pressure transensor for implanting in the eye. IEEE Trans. Biomed. Eng 14 74–83 1967. [PubMed: 6078978]
6. Cooper RL, Beale D. Constable IJ. Passive radiotelemetry of intraocular pressure in vivo: calibration and validation of continual scleral guard-ring applanation transensors in the dog and rabbit. Invest. Ophthalmol. Vis Sci 18 930–938 1979. [PubMed: 478782]
7. Downs JC, Burgoyne CF, Seigfreid WP, Reynaud JF, Strouthidis NG, Sallee V. 24-hour IOP telemetry in the nonhuman primate: implant system performance and initial characterization of IOP at multiple timescales. Invest. Ophthalmol. Vis. Sci 52 7365–7375. 2011. [PubMed: 21791586]
8. Frampton P, Da Rin, Brown B. Diurnal variation of intraocular pressure and the overriding effects of sleep. Am. J. Optom. Physiol. Opt 64 54–61. 1987. [PubMed: 3826279]
9. Greene ME, Gilman BG. Intraocular pressure measurement with instrumented contact lenses. Invest. Ophthalmol 13 299–302 1974. [PubMed: 4818815]
10. Heijl A, Leske MC, Bengtsson B, Hyman L, Bengtsson B, Hussein M. Reduction of intraocular pressure and glaucoma progression: results from the Early Manifest Glaucoma Trial. Arch. Ophthalmol 120 1268–1279. 2002. [PubMed: 12365904]
11. Ho JS, Yeh AJ, Neofytou E, Kim S, Tanabe Y, Patlolla B, Beygui RE, Poon AS. Wireless power transfer to deep-tissue microimplants. Proc Natl Acad Sci. 111 7974–9. 2014. [PubMed: 24843161]
12. IEEE Standard for Safety Levels with Respect to Human Exposure to Radio Frequency Electromagnetic Fields, 3kHz to 300 GHz. IEEE C95.1–1991 1999.
13. Leske MC, Connell AM, Wu SY, Hyman LG and Schachat AP Risk factors for open-angle glaucoma: the Barbados Eye Study. Arch. Ophthalmol 113 918–924. 1995. [PubMed: 7605285]

14. Li R and Liu JH. Telemetric monitoring of 24 h intraocular pressure in conscious and freely moving C57BL/6J and CBA/CaJ mice. Mol. Vision 14 745–749. 2008.
15. Liu JH, Kripke DF, Twa MD, Hoffman RE, Mansberger SL, Rex KM, Girkin CA, Weinreb RN. Twenty-four-hour pattern of intraocular pressure in the aging population. Invest Ophthalmol Vis Sci. 40 2912–2917. 1999. [PubMed: 10549652]
16. Liu JH, Zhang X, Kripke DF, Weinreb RN. Twenty-four-hour intraocular pressure pattern associated with early glaucomatous changes. Invest. Ophthalmol. Vis. Sci 44 1586–1590. 2003. [PubMed: 12657596]
17. Mansouri K and Shaarawy T. Continuous intraocular pressure monitoring with a wireless ocular telemetry sensor: initial clinical experience in patients with open angle glaucoma. Brit. J. Ophthalmol 95 627–629. 2011. [PubMed: 21216796]
18. Mansouri K, Medeiros FA, Tafreshi A, Weinreb RN. Continuous 24-hour monitoring of intraocular pressure patterns with a contact lens sensor: safety, tolerability, and reproducibility in patients with glaucoma. Arch. Ophthalmol 130 1534–1539. 2012.
19. McLaren JW, Brubaker RF, and Fitzsimon JS. Continuous measurement of intraocular pressure in rabbits by telemetry. Invest. Ophthalmol. Vis. Sci 37 966–975. 1996. [PubMed: 8631640]
20. Melki S, Todani A, Cherfan G. An implantable intraocular pressure transducer: initial safety outcome. JAMA Ophthalmol. 132 1221–1225. 2014. [PubMed: 24970583]
21. Montgomery KL, Yeh AJ, Ho JS, Tsao V, Mohan Iyer S, Grosenick L, Ferenczi EA, Tanabe Y, Deisseroth K, Delp SL, Poon AS. Wirelessly powered, fully internal optogenetics for brain, spinal and peripheral circuits in mice. Nat. Methods 12 969–74. 2015. [PubMed: 26280330]
22. Moore CG, Elaine C Johnson, and John C. Morrison. Circadian rhythm of intraocular pressure in the rat. Curr. Eye Res 15 185–191. 1996. [PubMed: 8670727]
23. RamRakhyani AK, Mirabbasi S, Chiao M. Design and Optimization of Resonance-Based Efficient Wireless Power Delivery Systems for Biomedical Implants. IEEE Trans. Biomed. Circ. Sys 5 48–63. 2011.
24. Refinetti R; Ma H; Satinoff E Body temperature rhythms, cold tolerance, and fever in young and old rats of both genders. Exp. Gerontol 25:533–543. 1990. [PubMed: 2097169]
25. Todani A, Behlau I, Fava MA, Cade F, Cherfan DG, Zakka FR, Jakobiec FA, Gao Y, Dohlman CH, Melki SA. Intraocular pressure measurement by radio wave telemetry. Invest. Ophthalmol. Vis. Sci 52 9573–9580. 2011. [PubMed: 22039243]
26. Walter P Development of a completely encapsulated intraocular pressure sensor. Ophthalmic Res. 32 278–84. 1999.
27. Wang G, Liu W, Sivaprakasam M, Zhou M, Weiland JD, Humayun MS. A dual band wireless power and data telemetry for retinal prosthesis. Conf. Proc. IEEE Eng. Med. Biol. Soc 1 4392–4395. 2006. [PubMed: 17946243]
28. Wentz CT, Bernstein JG, Monahan P, Guerra A, Rodriguez A, Boyden ES. A wirelessly powered and controlled device for optical neural control of freely-behaving animals. J. Neural Eng 8 046021 2011. [PubMed: 21701058]
29. Wilensky JT. Diurnal variations in intraocular pressure. Trans. Am. Ophthalmol. Soc 89 757–790. 1991. [PubMed: 1687295]

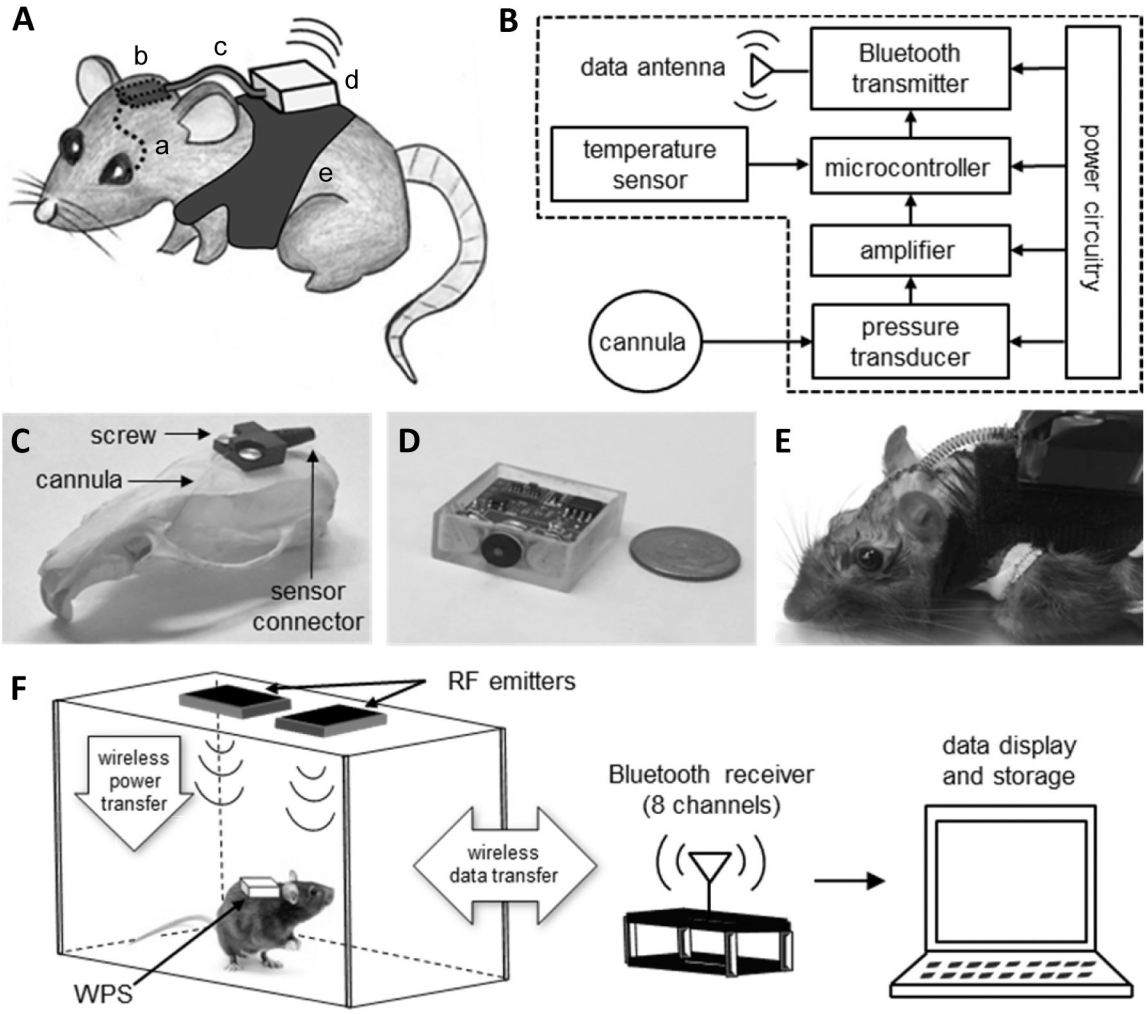

Figure 1.

IOP telemetry system. (A) Component illustration. a: cannula implanted in anterior chamber of eye, b: coupler affixed to skull, c: spring-encased tubing, d: pressure sensor electronics, e: vest on which sensor mounts. (B) Electronics diagram. IOP signal is conducted by the cannula to a pressure transducer, amplified, digitized by a microcontroller, and transmitted wirelessly with temperature data to a PC. The electronics are powered by two different circuits. For the BRS version of the system the powering circuitry is a regulated coin-cell battery. For the WPS version it consists of a RF antenna, RF harvester, and energy storage unit. (C) Picture of coupler affixed to a rat skull with screws. The cannula is inserted in the front port, the tubing is connected to the back port, and the coupler is covered in bone cement. (D) Picture of the wireless pressure sensor. The WPS version is shown but the BRS version has the same size and look. (E) Picture of an implanted rat outfitted with the BRS. (F) Illustration of the WPS setup. Two RF emitters atop the rat's cage provide constant power to sensor electronics via the RF energy harvesting circuit. The BRS setup is the same without the RF emitters. IOP data from up to 8 rats can be sent wirelessly via Bluetooth to a nearby PC.

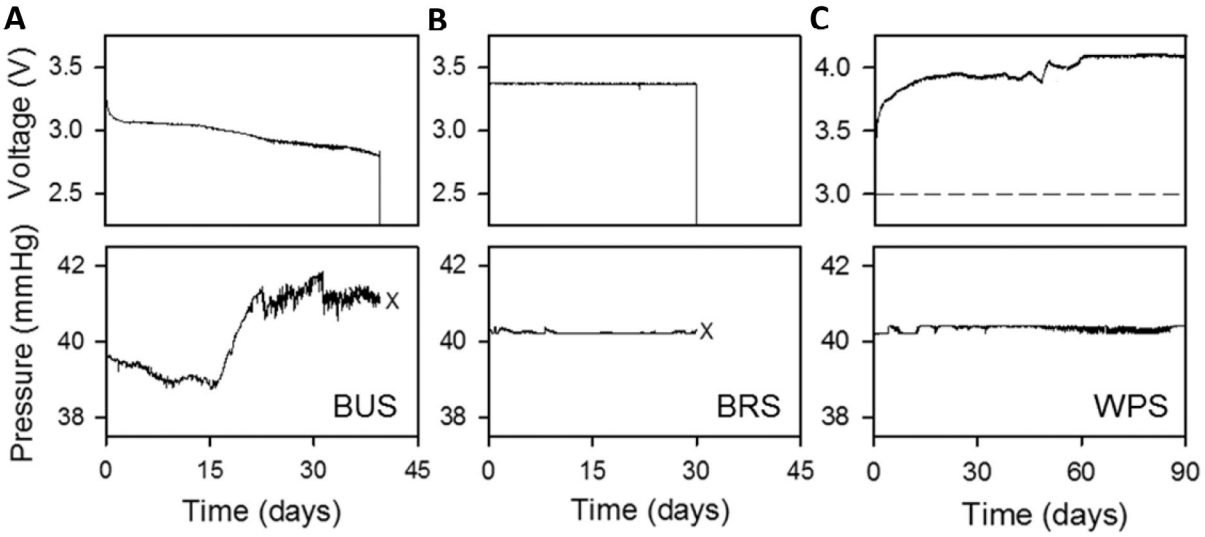

Figure 2.

Telemetry system powering. Constant hydrostatic pressure of 40 mmHg was applied to the system powered by: (A) unregulated 3V battery [BUS], (B) circuit-regulated 3V battery [BRS], and (C) wireless energy harvesting circuit [WPS]. Stored voltage (top) and pressure sensor output (bottom) of the system were recorded every 4 sec for several weeks. Linear regression of pressure data in B and C gave an offset of 40.1 and 40.4 mmHg and a slope of 0.119 and 0.002 mmHg/week, respectively. Crosses indicate battery failure and system shut down, which happened at 39 days in A and 30 days in B. The shutdown time depends on data collection rate. Batteryless system in C harvests energy from an external plugged-in RF emitter (height = 20 cm) and only shuts down if stored voltage falls below a minimum level (dashed line) needed for circuit operation.

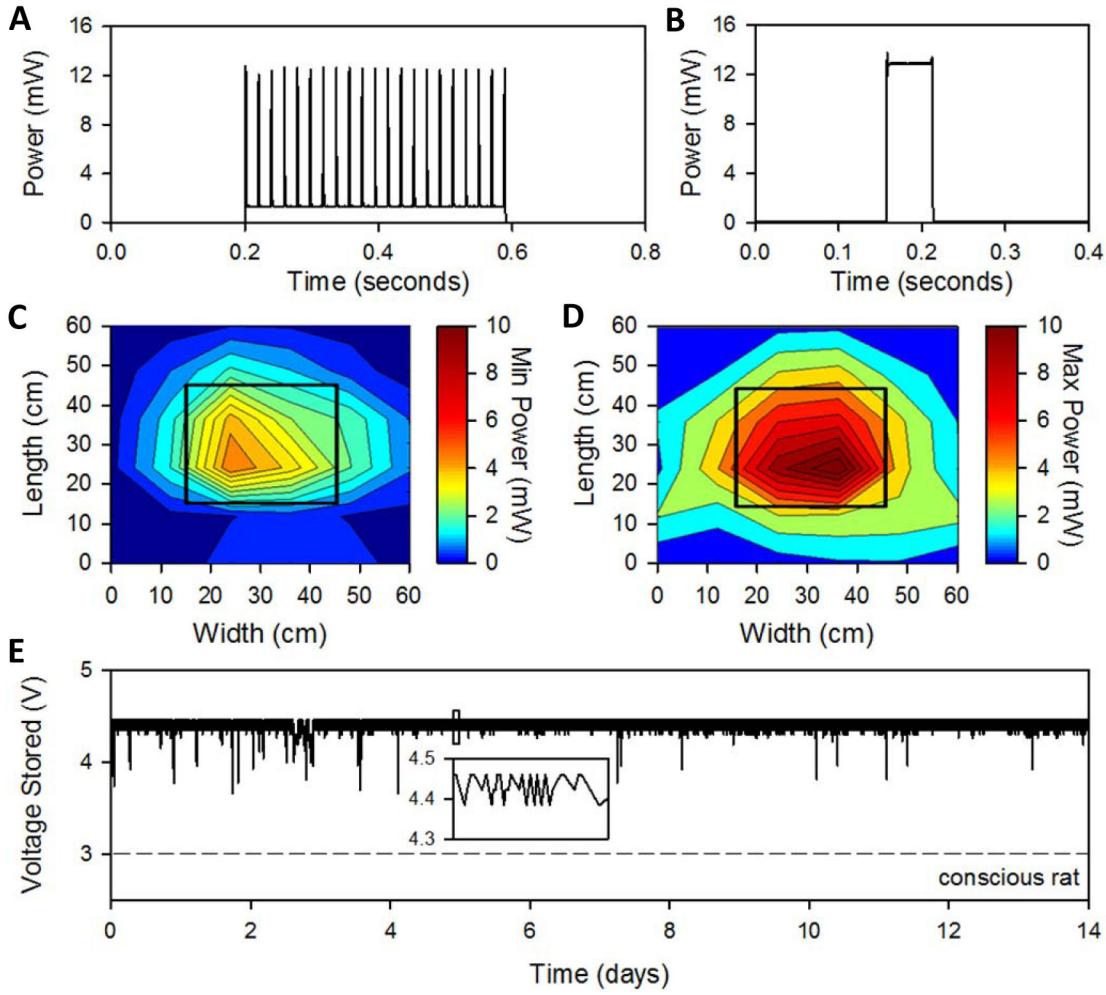

Figure 3.

Power transfer characteristics of WPS. (A) Power consumption profile during collection of one IOP and temperature measurement, given by the average of 20 readings in a 0.4 s period. (B) Consumption profile during wireless transmission of IOP and temperature data. (C) Map of minimum power reception level of the WPS across space with RF emitters centered 20 cm above. Thick line outlines the cage walls. (D) Map of maximum power reception level of the WPS with RF emitters in the same location. (E) Stored voltage level over a 2-week period with the system on an awake behaving rat. IOP data were collected every 4 s during the recording. Figure inset shows a 7-min segment of the voltage record. Dashed line marks the minimum voltage level needed to run system.

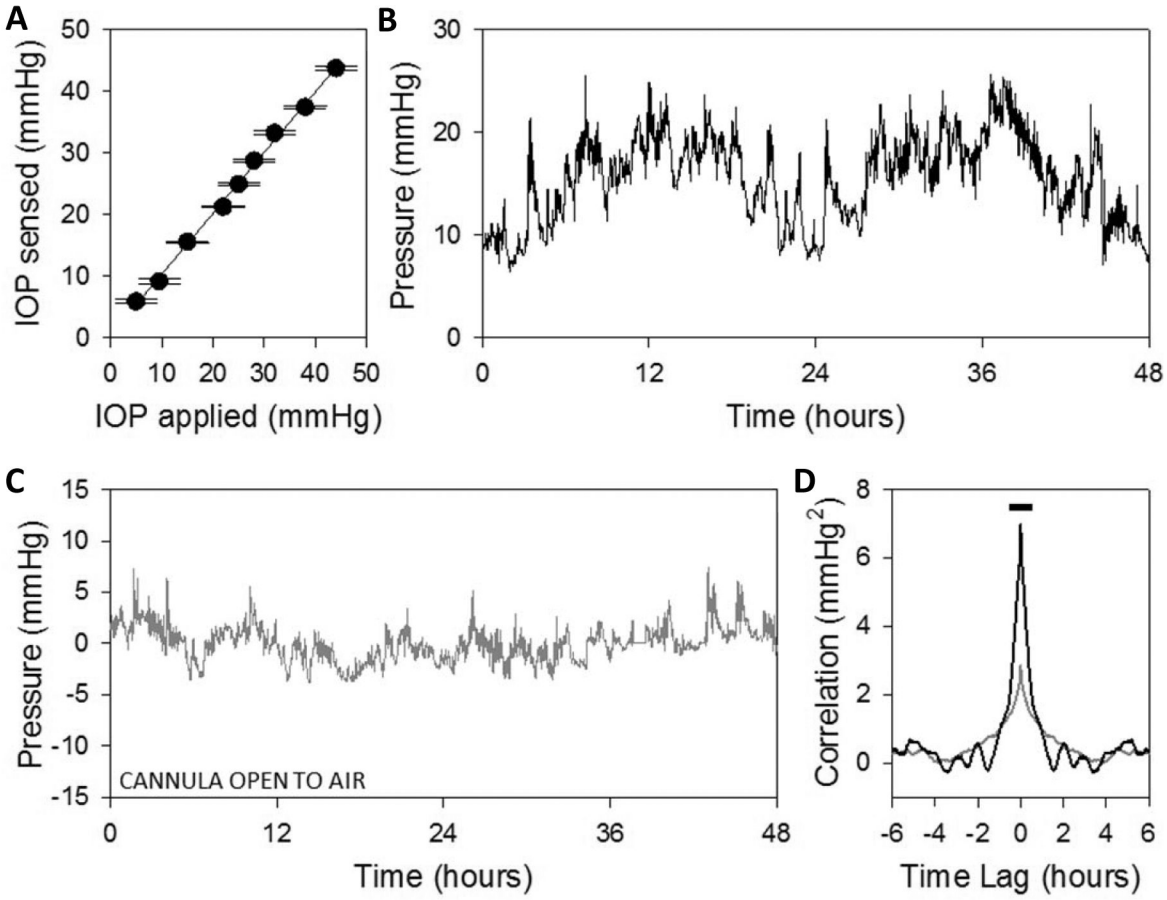

Figure 4.

System properties in live animals. (A) Pressure measured by the wireless sensor as IOP of an anesthetized rat was stepped to different levels by manometry via a needle inserted in the eye. Solid line is a linear regression fit of the data (n=3). (B) Pressure recorded by the wireless sensor over a 48-hr period in an awake behaving animal (rat j29). (C) Pressure record from the same animal in B after cutting the cannula outside the eye and opening it to air. Residual variations in the pressure record reflect hydrodynamic changes caused by head elevation and rotation. (D) Autocorrelation of the pressure signals in B (black) and C (grey). Bar marks ±30 min interval during which signals show strong positive correlation.

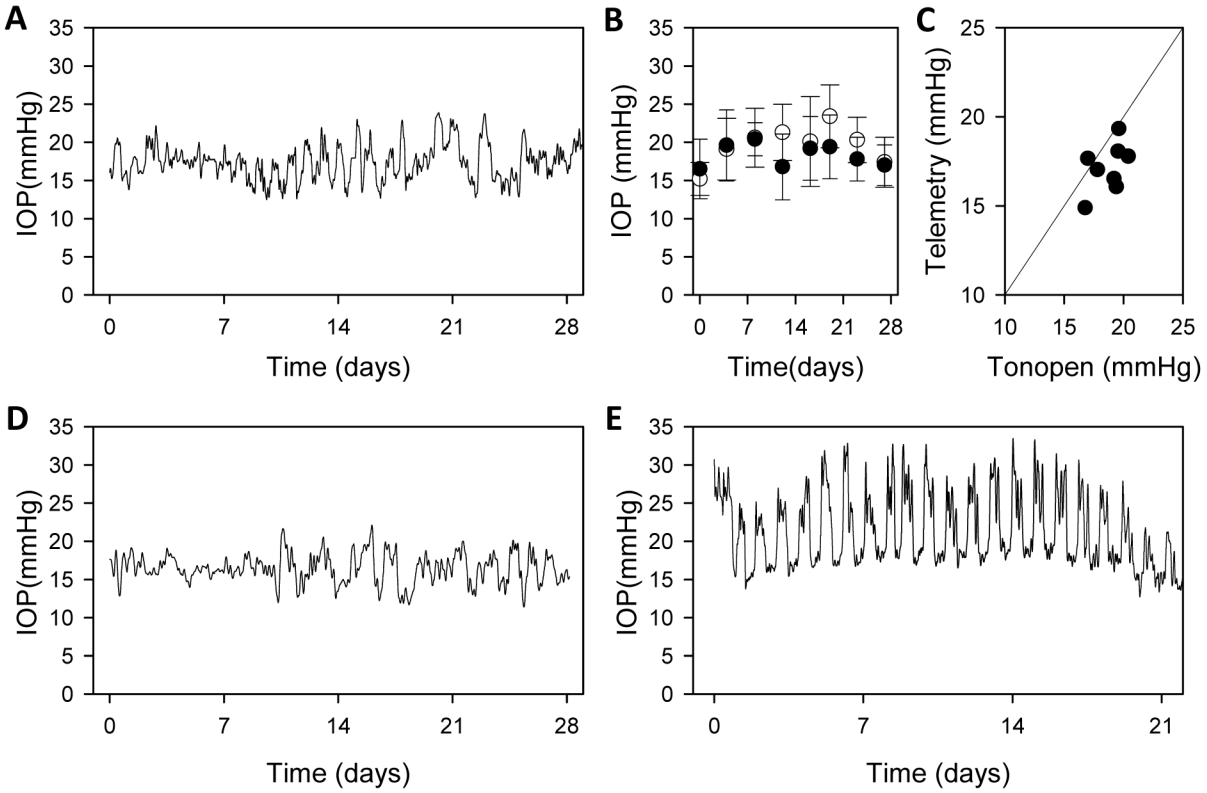

Figure 5.

Round-the-clock IOP recording in awake behaving rats. (A) Smoothed IOP record obtained with the telemetry system from an animal implanted over a month (rat j26). (B) IOP of the implanted (solid circles) and non-implanted (open circles) eye measured by tonometry from animal in A. Error bars give SD of 6 tonometry measurements. (C) Comparison of mean tonometer and telemetry data while tonometry data were collected (R = 0.5). (D, E) Smoothed IOP records from animal eyes that exhibited little temporal patterning (rat j22) and pronounced rhythmicity (rat j39), respectively

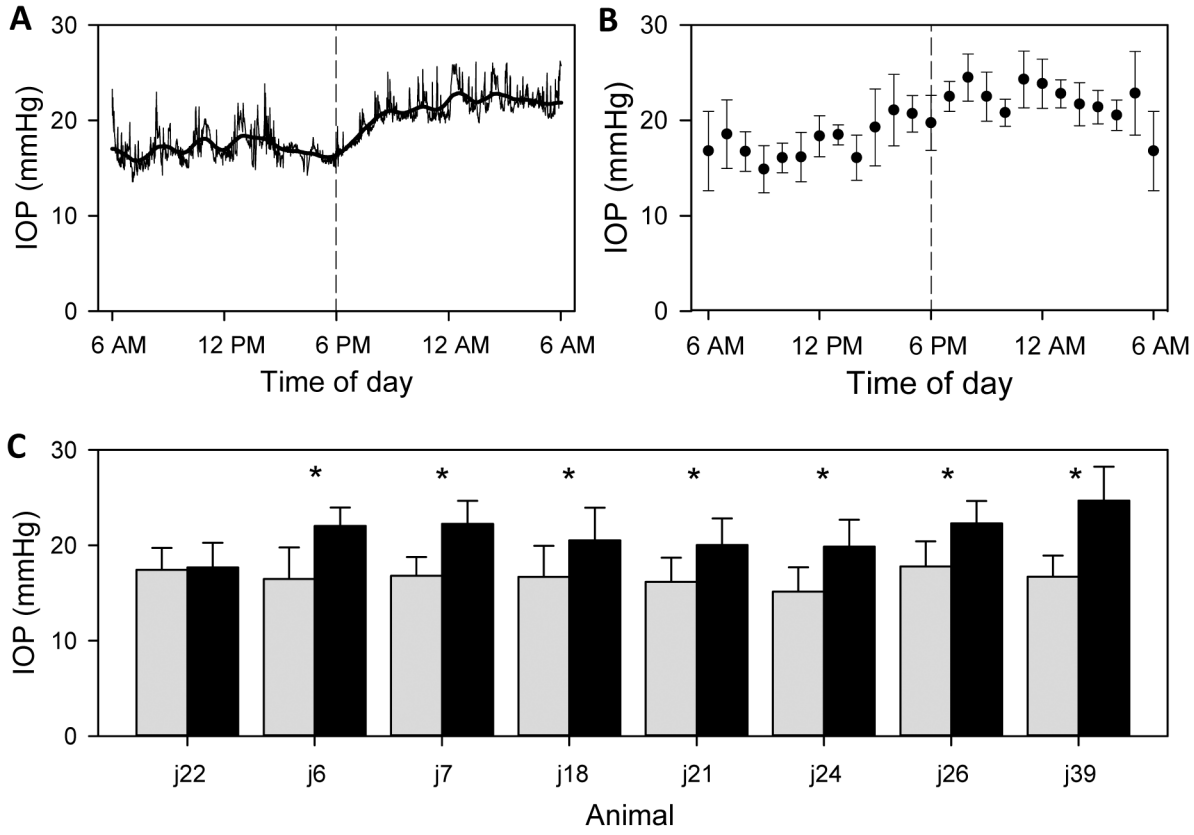

Figure 6.

Circadian IOP rhythm in rats. (A) Raw (thin line) and smoothed (thick line) IOP record over a 24-hr period from an awake behaving animal (rat j18) (B) Average IOP rhythm in one-hour bins (n = 7 days). Grey and black bars in A and B indicate timing of light-dark cycle to which the animal was exposed. (C) Average IOP during day (grey) and night (black) phases of the light-dark cycle for all implanted animals. Asterisks indicate daytime and nighttime IOP levels that differed significantly.

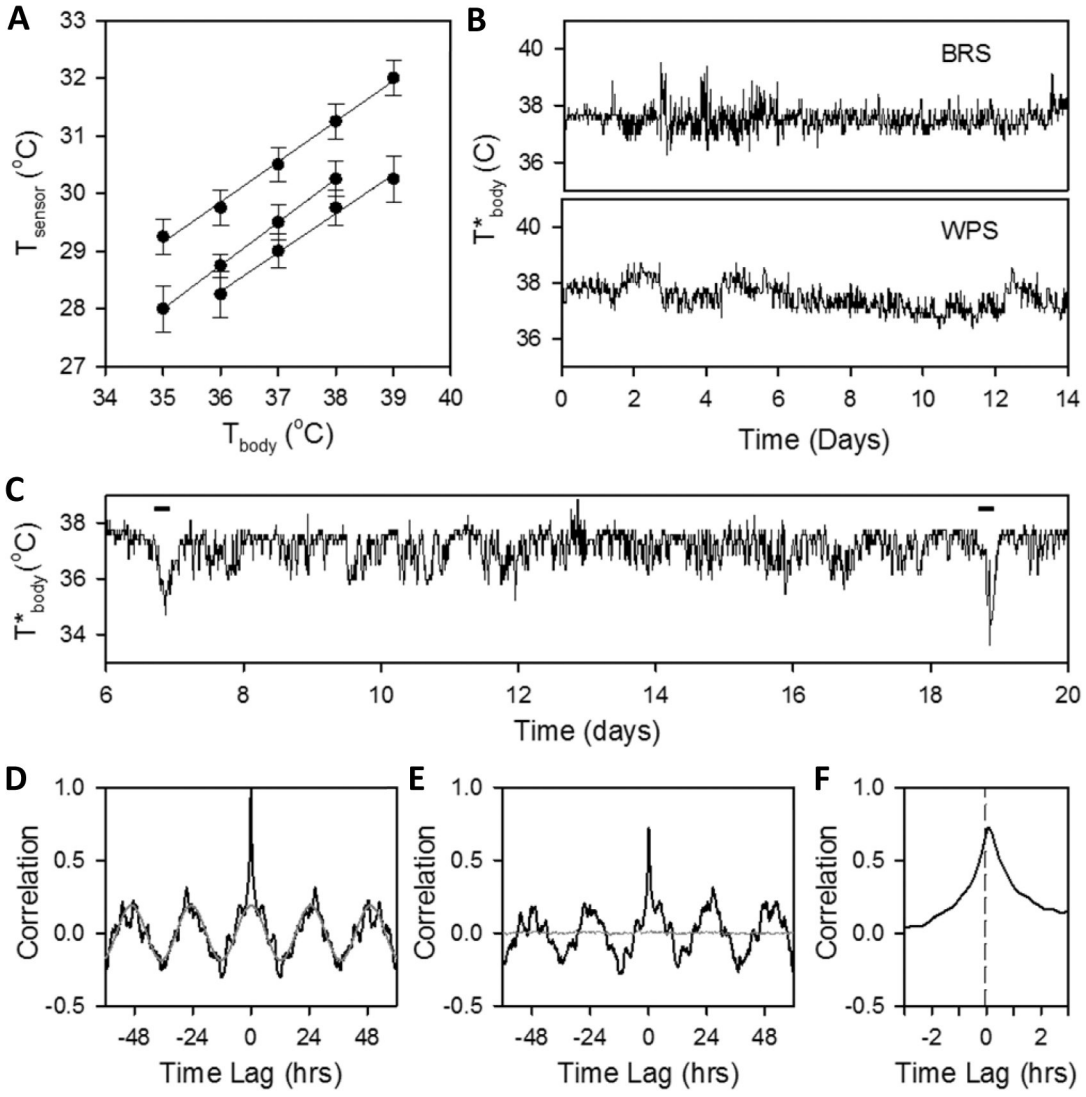

Figure 7.

Temperature measurements with the telemetry system. (A) Calibration data relating system sensor readings (T_{sensor}) to core body temperature (T_{body}) measured with a rectal thermometer from anesthetized rats outfitted with the system. Bars give standard deviation. (B,C) Temperature data recorded over two weeks from conscious rats by the BRS and WPS. Data were calibrated as shown in A to estimate body temperature (T^*_{body}). Bars indicate times when the rat was briefly anesthetized. (D) Auto-correlation of temperature record in C (rat j18). Grey line is sinewave fit to data (amplitude: 0.18, period: 24.64, phase: 1.57). (E) Cross-correlation of temperature record with IOP record of the same rat. Grey line gives correlation with randomly shuffled IOP record. (F) Cross-correlation data in E expanded in time scale. Positive lag corresponds to a lead in temperature.

Table 1.

Specifications of IOP telemetery system

Version	IOP Accuracy (mmHg)	IOP Noise (mmHg)	IOP Drift (mmHg/week)	Sample Rate (Hz)	Battery Life (days)
BRS	± 0.27	± 0.18	0.010 ± 0.024	0.25	28 ± 3
WPS	± 0.27	± 0.15	0.002 ± 0.001	0.25, 250	unlimited

Table 2:

Summary of WPS performance in conscious rats with RF energy emitters at cage height.

Experiment	Median Stored Voltage	Low Power Events	Max Down Time	Median Data Burst Interval
1	4.4 V	0	0 min	1.8 min
2	4.3 V	2	33 min	9.9 min
3	4.4 V	0	0 min	2.3 min